RESEARCH ARTICLE

Metabolomics responses and tolerance of *Pseudomonas aeruginosa* under acoustic vibration stress

Nawaporn Vinayavekhin[1,2]*, **Thanyaporn Wattanophas**[1], **Mark Francis Murphy**[3], **Alisa S. Vangnai**[2,4], **Glyn Hobbs**[3]

1 Center of Excellence in Natural Products Chemistry, Department of Chemistry, Faculty of Science, Chulalongkorn University, Bangkok, Thailand, 2 Center of Excellence in Biocatalyst and Sustainable Biotechnology, Faculty of Science, Chulalongkorn University, Bangkok, Thailand, 3 School of Pharmacy and Biomolecular Sciences, Liverpool John Moores University, Liverpool, United Kingdom, 4 Department of Biochemistry, Faculty of Science, Chulalongkorn University, Bangkok, Thailand

* nawaporn.v@chula.ac.th

Abstract

Sound has been shown to impact microbial behaviors. However, our understanding of the chemical and molecular mechanisms underlying these microbial responses to acoustic vibration is limited. In this study, we used untargeted metabolomics analysis to investigate the effects of 100-Hz acoustic vibration on the intra- and extracellular hydrophobic metabolites of *P. aeruginosa* PAO1. Our findings revealed increased levels of fatty acids and their derivatives, quinolones, and *N*-acylethanolamines upon sound exposure, while rhamnolipids (RLs) showed decreased levels. Further quantitative real-time polymerase chain reaction experiments showed slight downregulation of the *rhlA* gene (1.3-fold) and upregulation of *fabY* (1.5-fold), *fadE* (1.7-fold), and *pqsA* (1.4-fold) genes, which are associated with RL, fatty acid, and quinolone biosynthesis. However, no alterations in the genes related to the *rpoS* regulators or quorum-sensing networks were observed. Supplementing sodium oleate to *P. aeruginosa* cultures to simulate the effects of sound resulted in increased tolerance of *P. aeruginosa* in the presence of sound at 48 h, suggesting a potential novel response-tolerance correlation. In contrast, adding RL, which went against the response direction, did not affect its growth. Overall, these findings provide potential implications for the control and manipulation of virulence and bacterial characteristics for medical and industrial applications.

Introduction

Microorganisms are known to adapt their transcript, protein, or metabolite production in response to various stimuli and stresses in their environment for survival [1, 2]. The stimuli that have been extensively studied are primarily chemicals, including cell-to-cell communication signals used to manipulate organisms [3], as well as toxic chemicals or solvents used for the bioremediation of contaminants or as starting materials for biosynthesis [1]. In addition to

these chemical stimuli, the mechanisms of microbial responses to other environmental conditions, such as changes in light, temperature, salinity, pH, and nutrient availability, have also been elucidated, as they have the ability to modulate microbial growth, virulence, and metabolite production [4–8].

Another stimulus that affects microbial physiology is acoustic vibration or sound waves. Studies have shown that acoustic vibration can alter various aspects of microbial behavior, including growth, antibiotic susceptibility, membrane permeability, intracellular calcium and potassium ion concentrations, and synthesis of RNA and proteins in *Chromobacterium violaceum*, *Escherichia coli*, *Serratia marcescens*, *Staphylococcus aureus*, *Streptococcus pyogenes*, *Saccharomyces cerevisiae*, and *Candida albicans* [9–11]. Metabolites linked to the quorum-sensing (QS) process, such as violacein and prodigiosin, were also found to differ in their amounts in sound-exposed samples of *Chromobacterium violaceum* and *Serratia marcescens*, respectively, as estimated by ultraviolet absorption [9]. Additionally, significant differences in volatile metabolite profiles were observed in *Saccharomyces cerevisiae* undergoing sound treatment [12]. Further studies have suggested that the direction and magnitude of these changes in microbial characteristics may depend on factors, such as the type of microorganism, frequency of the sound (either a single frequency or multiple frequencies in music), and intensity of the sound [9, 10, 13]. However, despite these findings, our understanding of microbial responses to acoustic vibration is still in its infancy, with a limited investigation into the chemical and molecular basis of these responses.

Pseudomonas aeruginosa is a ubiquitous Gram-negative opportunistic bacterial pathogen that is prevalent in most hospitals [14]. It can cause serious illness in patients on ventilators, as well as those with cystic fibrosis, burns, cancer, and immunodeficiency [15]. Its intricate QS communication networks are composed of at least three interconnected systems: Las, Rhl, and PQS [16]. In the Las and Rhl systems, the enzymes LasI and RhlI catalyze the synthesis of the signaling molecules *N*-(3-oxododecanoyl)-L-homoserine lactone (3-oxo-C_{12}-HSL) and *N*-butyryl-L-homoserine lactone (C_4-HSL), respectively [17–20]. Meanwhile, in the PQS system, the synthesis of 2-heptyl-3-hydroxy-4-quinolone, also known as the pseudomonas quinolone signal (PQS or C_n-PQS (7:0)), is mediated by the enzyme products of the *pqsABCD* and *pqsH* gene clusters [21, 22]. These autoinducer molecules bind to their transcriptional regulators, LasR, RhlR, and PqsR, to modulate the target promoters of the genes involved in various processes, such as cell-to-cell communication, virulence, rhamnolipid production, biofilm formation, and swarming motility [23]. The Las system is often perceived as being at the top of the hierarchy, regulating the Rhl system, which in turn controls the PQS system [16]. However, certain environmental factors have been demonstrated to act through global regulators that govern this QS network and override this hierarchical order [23].

Previous research has shown that *P. aeruginosa* responded to acoustic vibration by stimulating growth and enhancing biofilm formation [13]. When cultured in culture dishes on top of vibration sources at frequencies of 100, 800, and 1600 Hz for 48 h, *P. aeruginosa* exhibited 0.3-, 2.8-, and 2.6-fold increases in biofilm formation, respectively, compared to the silence control. Interestingly, the biofilm formed in a concentric ring pattern, potentially in accordance with the nodes and antinodes of the standing wave, and was found to be affected by the amplitude of vibration. However, as is the case with other microorganisms, a more comprehensive understanding of the observed phenotype is still needed in order to manipulate or exploit this species for medical and industrial applications.

Untargeted metabolomics is a comparative method used for the global profiling of metabolites [24]. As this method enables the simultaneous detection of broad classes of metabolites, it can provide unbiased information about metabolites and metabolic pathways involved in the

response to sound stimulus and help in deciphering a more comprehensive view of the mechanisms underlying the response.

Since previous research has demonstrated that 100 Hz vibration induces the smallest increase in biofilm formation in *P. aeruginosa* compared to other tested frequencies [13], we were interested in further exploring its effects at both the chemical and molecular levels. In this study, we employed untargeted metabolomics platforms to investigate changes in intracellular and extracellular hydrophobic metabolites in *P. aeruginosa* PAO1 (a laboratory reference strain) following a 48-h exposure to 100 Hz acoustic vibration, compared to a silence control. Subsequently, transcript levels of genes potentially associated with the alteration of metabolites were quantified using quantitative real-time polymerase chain reaction (qRT-PCR). Lastly, in order to better understand the adaptation, the effects of these metabolites on the growth fitness of *P. aeruginosa* under sound exposure were also evaluated.

Materials and methods

Vibration system and chemicals

A 100-Hz acoustic vibration was generated from a programmed Arduino board (serving as a sinusoidal waveform generator) connected to a 45-mm 0.2-W super-thin Mylar speaker, as previously employed [13]. Beef extract, yeast extract, and peptone were from HiMedia (Maharashtra, India). NaCl was from Ajax Finechem-Thermo Scientific (Rockford, IL, USA). $CHCl_3$ was from RCI Labscan (Bangkok, Thailand). MeOH and ammonium hydroxide (25%) were from Merck (Rahway, NJ, USA). Isopropanol was obtained from Honeywell (Charlotte, NC, USA). Formic acid was from Sigma-Aldrich (Milwaukee, WI, USA). Rhamnolipids (R90; 90%) were obtained from AGAE Technologies-Sigma-Aldrich (Milwaukee, WI, USA), and sodium oleate from Tokyo Chemical Industry (Tokyo, Japan). All chemicals were reagent grade or liquid chromatography grade or better as appropriate and used as supplied.

Bacterial strains and growth conditions

Pseudomonas aeruginosa PAO1 was kindly provided by Professor Junichi Kato, Hiroshima University. Bacteria were grown aerobically at 150 or 200 rpm, 30°C for 16–18 h in nutrient broth (NB; 1 g L^{-1} beef extract, 2 g L^{-1} yeast extract, 5 g L^{-1} peptone, and 5 g L^{-1} NaCl, pH 7.4) as reported previously [13]. The overnight cultures were diluted in fresh NB medium to an optical density at 600 nm (OD_{600}) of 0.45–0.50. For metabolomics and qRT-PCR analyses, 20 mL of diluted culture was then added to each 60-mL culture bottle. For metabolite addition assay, the diluted culture was supplemented with indicated concentrations of metabolites or solvent vehicle (water) as control, before 1 mL was added to each 4-mL culture glass vial. Subsequently, the cultures were allowed to grow statically at 30°C with (on top of the speaker in an incubator) or without (in a separate incubator) 100 Hz acoustic vibration treatment for a predetermined time as indicated.

Metabolites extraction

Metabolites extraction protocols were modified from those described previously [25]. After incubation with or without acoustic vibration for 48 h, bacterial cultures were vortexed briefly and vigorously to mix, and 700 μL of cultures were collected for OD_{600} measurement. The remaining cultures were then centrifuged at 4,472*g*, 4°C for 15 min to separate bacterial cells and supernatant. The cell pellets were washed once with 20 mL of NB medium, resuspended in 3 mL of NB medium, and extracted with a mixture solution of 6 mL $CHCl_3$ and 3 mL MeOH. The supernatant was extracted with a solution of 10 mL $CHCl_3$ and 5 mL MeOH.

Subsequently, the mixtures were centrifuged at 1,000g, 4˚C for 5 min. The organic layer was collected, dried under a stream of nitrogen gas, and stored at 20˚C. The samples were reconstituted in 200 μL CHCl$_3$ before liquid chromatography (LC)–mass spectrometry (MS) analysis.

LC–MS and LC–MS/MS analyses

40 μL of each sample was analyzed in both the positive and negative ion modes on an Ultimate DGP-3600SD LC coupled to a Bruker MicrOTOF Q-II MS instrument, as previously described [26]. However, some parameters were modified slightly to obtain optimal spectra. Specifically, the collision RF was set at 250 Vpp. The active exclusion was set to release ions after 0.30 min. Collision energies for ions with charge = 1 were set at 20 eV for m/z 500.00, 30 eV for m/z 1000.00, and 40 eV for m/z 2000.00. For other m/z values, the collision energies were automatically interpolated from those of the closest m/z values.

LC–MS untargeted data analysis

The total ion chromatograms of the 100 Hz-exposed and unexposed control groups were obtained in two independent sets of triplicates, totaling 12 chromatograms for intracellular pellet samples and 12 chromatograms for extracellular supernatant samples in each ion mode. The comparative data analyses were then performed separately for the intracellular and extracellular samples, as described previously [26]. However, the criteria for identifying metabolite ions with altering levels upon exposure to 100-Hz vibration were changed to (i) a minimum fold change of ≥ 2, instead of ≥ 4, as there were no observable differences in OD$_{600}$ of the two groups, and (ii) the minimum integrated mass ion intensity (MSII) in the elevated sample groups of 10,000, instead of 30,000, to allow for the depiction of more metabolites. The metabolite ions (defined by m/z and retention time) were included in the final list of changed metabolite ions only if they passed through the imposed filters for both sets of experiments.

qRT-PCR analysis

1.5 mL of each *P. aeruginosa* culture was centrifuged at 16,000g for 1 min to collect cell pellets. Total RNA was isolated immediately from the cell pellets using an easy-spin^{TM} [DNA free] total RNA extraction kit (Intron Biotechnology, Seongnam, South Korea). In the last step, the total RNA was eluted from the binding column using 50 μL of RNase-free water. Subsequently, 1 μL of the total RNA was converted to cDNA using a Maxime RT premix kit with random primers (Intron Biotechnology). The obtained cDNA solution was then diluted 20-fold and used as a template in the qRT-PCR analysis using RealMOD^{TM} Green W^2 2x qPCR mix (Intron Biotechnology). The primer sequences (Bionics, Seoul, South Korea) for the amplification of the target and internal control (*proC* and *rpoD*) genes [27] are listed in S10 Table of S1 File. The final concentration of each primer was 0.5 μM. The annealing temperature was 60˚C, and the elongation time was 20 s. Unless specified earlier, all kits were applied according to the manufacturer's instructions. Finally, the 2$^{-\Delta\Delta Ct}$ method was used to calculate the relative mRNA expression levels of the target genes in the 100-Hz-exposed sample *vs*. the unexposed control. Student's *t*-test was then applied to determine the statistical significance of the ΔC_t values between the sample groups, and only those with $p < 0.05$ were considered significant.

Metabolite addition assay

For the construction of growth curves, the whole culture in each vial with or without 2 mM or 10 mM of sodium oleate, or 1.2 g L^{-1} or 6 g L^{-1} of rhamnolipids was collected at 6, 9, 24, or 48 h after incubation in the presence or absence of 100-Hz vibration. The sample was mixed by

vortex to obtain a homogeneous culture, and the cell density was determined by OD_{600}. Experiments were performed in triplicates or quadruplicates.

Results

Untargeted metabolomics of *P. aeruginosa* PAO1 under 100-Hz vibration

As previous work reported a slight enhancement in biofilm formation in *P. aeruginosa* PAO1 when grown in NB medium and exposed to 100 Hz acoustic vibration for 48 h [13], this condition was selected for detecting changes in metabolite composition and levels using untargeted metabolomics analysis. However, to ensure a consistent sound treatment condition for all three cultured replicates, PAO1 was cultured in glass bottles instead of Petri dishes used previously, allowing them to be placed simultaneously and symmetrically on top of a speaker connected to a vibration generator. The 100 Hz-exposed and unexposed cultures were incubated in separate incubators to maintain a silent environment for the control. Two independent sets of untargeted metabolomics analyses were also conducted to account for random factors and ensure the reproducibility of the detected changes in metabolite levels. After 48 h of incubation with or without sound, some cells were aggregated at the bottom, but no biofilm could be observed in any cultures. Subsequently, hydrophobic metabolites were extracted separately for the intra- (cell pellet) and extracellular (supernatant) components using a 2:1 (*v/v*) mixture of chloroform to methanol. The concentrated extracts were then analyzed using the LC–MS-based untargeted metabolomics platforms [25, 26].

To identify metabolites associated with 100 Hz vibration responses, relative levels of metabolite ions detected in the 100 Hz-treated and untreated LC–MS chromatograms were obtained using an XCMS program [28] and normalized by the OD_{600} value of each sample to eliminate slight variations in growth. The normalized levels of each metabolite ion in the treated samples were then compared with those in the untreated samples by calculating the fold changes. As no statistical difference was observed in the growth of the 100 Hz-treated and untreated *P. aeruginosa* cultures, metabolite ions were considered potentially associated with the vibration responses if their levels were increased or decreased by at least twofold with statistical significance (determined by Student's *t*-test with $p < 0.05$). Using these criteria, 3 and 5 extracellular, and 12 and 37 intracellular metabolite ions were found to be increased, whereas 24 and 29 extracellular, and 1 and 0 intracellular metabolite ions were found to be decreased in the 100 Hz-treated samples in positive and negative ion modes, respectively, compared to the control without vibration (Fig 1 and S1–S7 Tables in S1 File).

Next, the chemical structures of the altered metabolite ions were manually characterized using accurate masses, previously reported retention time [25, 26], and tandem mass spectra (S1 Fig in S1 File). Out of the 111 metabolite ions with changed levels, probable structures could be assigned to 83 ions or 75%, which is relatively high for untargeted metabolomics analyses (S1–S7 Tables in S1 File). The results revealed elevated levels of fatty acids and their oxo derivatives in the extracellular components of the 100 Hz-treated samples compared to the silence controls, whereas monorhamnolipids (MRLs) and dirhamnolipids (DRLs) levels were found to decrease. Intracellularly, following 100 Hz sound treatment, the levels of fatty acids and their oxo and hydroxy derivatives were also increased, but their upregulation was accompanied by quinolones (2-alkyl-4-hydroxyquinoline *N*-oxide (AQNO), 2-alkyl-3-hydroxy-4-quinolone (C_n-PQS), and 2-alkyl-4-hydroxyquinoline (AHQ)) and *N*-acylethanolamine (NAE) (Table 1 and Fig 2 and S1–S7 Tables in S1 File). Using accurate masses and retention time, we also searched our datasets for some other known metabolites, including *N*-(3-oxodo-decanoyl)-L-homoserine lactone (3-oxo-C_{12}-HSL), phosphatidylethanolamine (PE), phosphatidylglycerol (PG), and diacylglycerol (DAG), and found that the levels of these metabolites
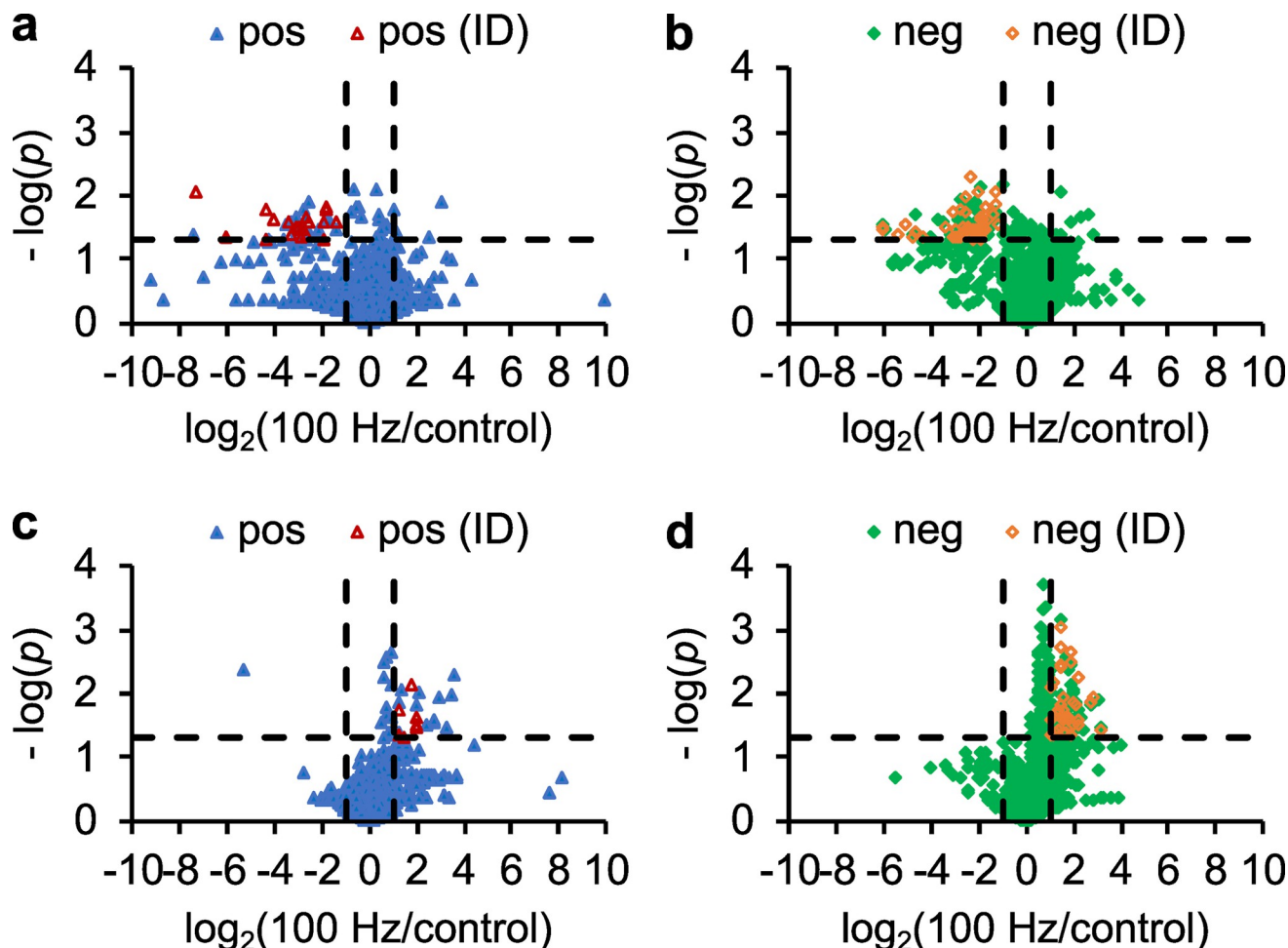
Fig 1. Volcano plots of differential metabolites in *Pseudomonas aeruginosa* at 48 h after 100-Hz acoustic vibration exposure. In the untargeted metabolomics analysis, the levels of each (a, b) extracellular and (c, d) intracellular metabolite ion in both the (a, c) positive (pos; *blue triangles*) and (b, d) negative (neg; *green diamonds*) ion modes were compared between sample groups with (100 Hz) or without (control) 100-Hz sound exposure. Each data point represents a metabolite ion with an average mass ion intensity (MSII) of at least 10,000 counts in the more abundant sample groups. Its p-value (p) from a Student's t-test is plotted against the fold change of the 100-Hz-treated group over the control. Ions above the horizontal dash line have a p-value of less than 0.05. Those located outside the right and left vertical dash lines exhibit relative levels at least 2-fold higher in the 100-Hz group compared to the control and *vice versa*, respectively. These ions are considered changed metabolite ions. The changed metabolite ions, pos(ID) and neg(ID), represent the structurally characterized positive-mode (pos) and negative-mode (neg) ions in this study, depicted with *red open triangles* and *orange open diamonds*, respectively. Characterization was achieved through a combination of accurate masses, previously reported retention times, and tandem mass spectra.

https://doi.org/10.1371/journal.pone.0297030.g001

changed either less than twofold or with statistical insignificance following acoustic vibration treatment, consistent with the results from untargeted analyses (Table 1 and S8 Table in S1 File). Lastly, metabolite standards of MRL, DRL, AHQ, C_n-PQS, and NAE were acquired, and their retention time and tandem mass spectra were compared to those detected in the bacterial samples, which together further supported the prior structural assignment of these compounds (Fig 2 and S1 Fig in S1 File).

Expression levels of genes in biosynthetic pathways of changed metabolites and related in *P. aeruginosa*

To decipher the mechanisms of acoustic vibration responses and to find the correlation between sound-stimulated metabolites and genes in their biosynthetic pathways, the

Table 1. Relative levels of represented extracellular and intracellular metabolites identified in the untargeted metabolomics analysis of *Pseudomonas aeruginosa* PAO1 grown statically with and without 100-Hz acoustic vibration treatment for 48 h.

Metabolite class and acyl chain			Ion	*m/z*	RT (min)	Fold[a, b]
Elevated metabolites in 100 Hz-treated extracellular samples						
	Fatty acid (FA)					
		16:1	[M–H]⁻	253.2198	19.4	13.5[†]
		18:1	[M–H]⁻	281.2509	20.2	9.2[†]
		oxo 16:1	[M–H]⁻	267.1972	17.4	3.6[*]
Decreased metabolites in 100 Hz-treated extracellular samples						
	Monorhamnolipid (MRL)					
		10:0/10:0	[M–H]⁻	503.3304	23.9	*8.0[†]*
		10:0/12:1	[M–H]⁻	529.3448	25.3	*7.4[‡]*
		10:0/12:0	[M–H]⁻	531.3601	26.2	*11.5[‡]*
	Dirhamnolipid (DRL)					
		10:0/10:0	[M–H]⁻	649.3862	23.7	*5.4[*]*
		10:0/12:1	[M–H]⁻	675.4021	25.0	*4.4[*]*
		10:0/12:0	[M–H]⁻	677.4191	25.9	*5.2[*]*
		12:0/12:0	[M–H]⁻	705.4486	28.2	*9.3[†]*
Elevated metabolites in 100 Hz-treated intracellular samples						
	Fatty acid (FA)[c]					
		16:0	[M–H]⁻	255.2336	19.7	3.4[‡]
		17:1	[M–H]⁻	267.2336	19.6	9.6[*]
		18:1	[M–H]⁻	281.2507	20.1	6.7[‡]
		19:1	[M–H]⁻	295.2653	20.3	7.3[‡]
		oxo 18:1	[M–H]⁻	295.2272	19.0	2.8[*]
		hydroxy 18:1	[M–H]⁻	297.2451	18.0	8.8[*]
		hydroxy 18:0	[M–H]⁻	299.2582	18.7	2.7[‡]
	Quinolines					
		AQNO (7:0)	[M–H]⁻	258.1484	13.7	2.3[*]
		AQNO (11:1)	[M–H]⁻	312.1961	18.1	2.8[*]
		C_n-PQS (9:0)	[M–H]⁻	286.1785	29.9	2.1[*]
		AHQ (9:1)	[M + H]⁺	270.1867	27.1	4.0[*]
		AHQ (9:0)	[M + H]⁺	272.2028	27.2	3.4[*]
	N-acylethanolamine (NAE)					
		17:1	[M–H]⁻	310.2700	36.3	3.0[‡]
		18:2	[M–H]⁻	322.2713	36.0	3.4[‡]
		18:1	[M–H]⁻	324.2870	37.6	3.2[*]
		19:1	[M–H]⁻	338.3017	38.1	3.0[*]
Other extracellular metabolites (fold < 2 or $p > 0.05$)						
	3-oxo-C_{12}-HSL		[M + H]⁺	298.2033	24.5	1.1
Other intracellular metabolites (fold < 2 or $p > 0.05$)						
	Phosphatidylethanolamine (PE)					
		16:0/18:1	[M–H]⁻	716.5180	44.7	1.1
		18:1/18:1	[M–H]⁻	742.5320	45.2	0.9
	Phosphatidylglycerol (PG)					
		16:0/18:1	[M–H]⁻	747.5151	39.2	1.0
		18:1/18:1	[M–H]⁻	773.5289	40.7	0.8
	Diacylglycerol (DAG)					
		16:0/18:1	[M + NH₄]⁺	612.5544	44.4	1.7[*]

(Continued)

Table 1. (Continued)

Metabolite class and acyl chain		Ion	m/z	RT (min)	Fold[a, b]
	18:1/18:1	$[M + NH_4]^+$	638.5699	44.7	1.6

Abbreviations: AHQ, 2-alkyl-4-hydroxyquinoline; AQNO, 2-alkyl-4-hydroxyquinoline N-oxide; C_n-PQS, 2-alkyl-3-hydroxy-4-quinolone; m/z, mass-to-charge ratio; 3-oxo-C_{12}-HSL, N-(3-oxododecanoyl)-L-homoserine lactone; RT, retention time

[a] Fold value represents the ratio of the average mass ion intensity of 100 Hz-treated samples and that of the control and vice versa (in italics)

[b] Student's t test:

[*], $p < 0.05$

[†], $p < 0.01$

[‡], $p < 0.005$; $N = 3$

[c] Only representative, most abundant ions are presented here (see S1–S7 Tables in S1 File for a complete list)

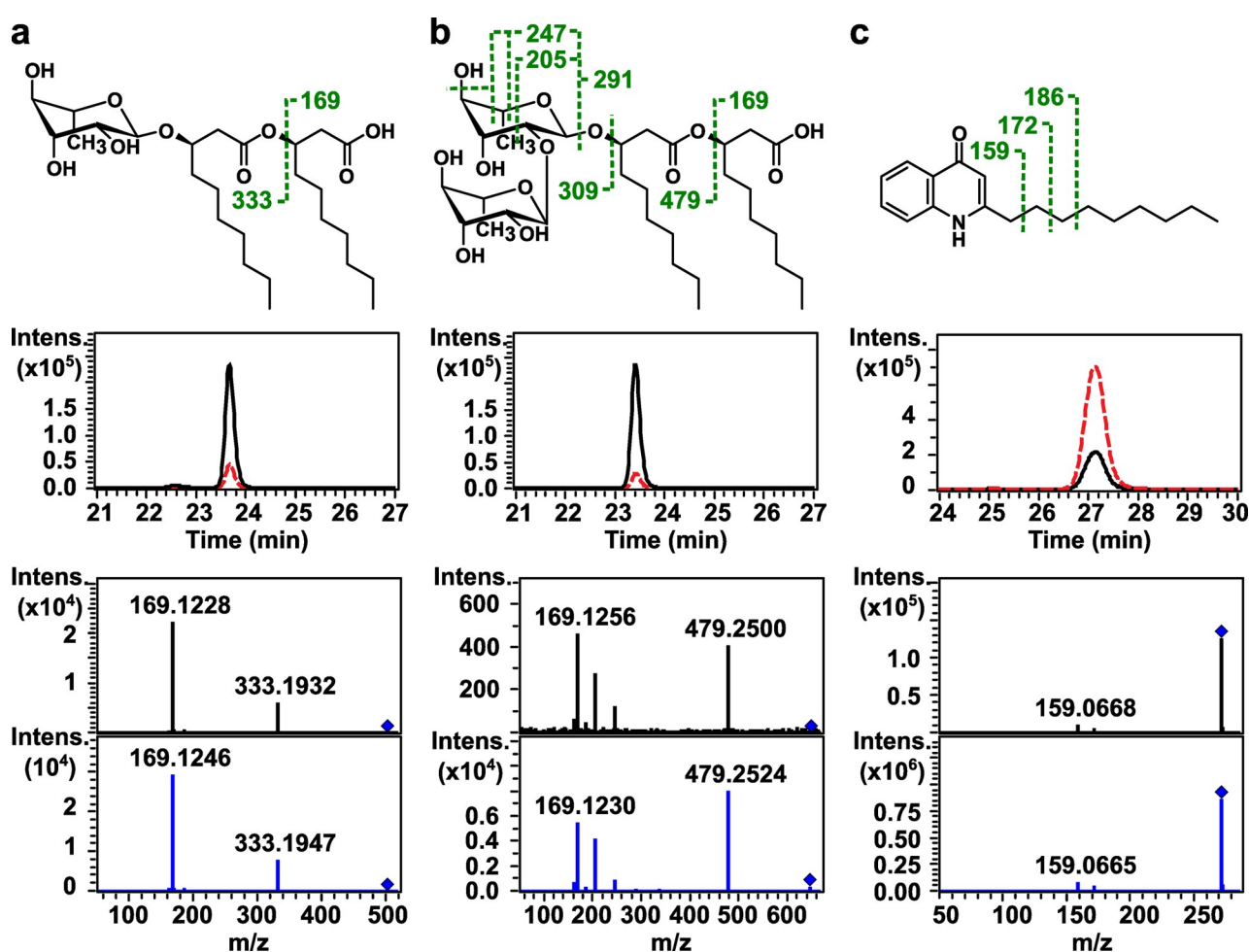https://doi.org/10.1371/journal.pone.0297030.t001

Fig 2. Chemical structures with proposed MS/MS fragments (top), extracted ion chromatograms (middle), and MS/MS spectra (bottom) of representative differential metabolites. The [M–H]⁻ions of the two most abundant detected rhamnolipids, (a) monorhamnolipid (10:0/10:0) and (b) dirhamnolipid (10:0/10:0), were decreased in their levels in the extracellular samples upon exposure to 100-Hz sound (middle; *black solid lines*), compared to the controls (middle; *red dashed lines*), whereas the [M + H]⁺ ion of (c) 2-alkyl-4-hydroxyquinoline (9:0) was elevated in its level in the intracellular samples. The structures of all representative metabolites were confirmed by comparing both the retention times and MS/MS spectra of samples (bottom; top spectra with *black lines*) with those of commercial standards (bottom; bottom spectra with *blue lines*). The proposed fragments observed in the MS/MS spectra are indicated with green dashed lines, along with the corresponding m/z values in the chemical structures.

https://doi.org/10.1371/journal.pone.0297030.g002

expression levels of related genes were determined by qRT-PCR analysis on the total mRNA isolated from *P. aeruginosa* PAO1 grown under the same conditions as those for the untargeted metabolomics experiments. Specifically, the relative mRNA expression levels were quantitated for genes in the *de novo* fatty acid synthase (*fabB, fabF, fabG, fabH3, fabI, fabV, fabY, fabZ*), the fatty acid β-oxidation (*fadB1, fadB4, fadB5, fadD1, fadD2, fadD4, fadE*), the rhamnolipid biosynthetic (*rhlA, rhlC, rhlY, rmlB*), and the quinolone biosynthetic (*pqsA, pqsH*) pathways (Fig 3) [29–36]. Although there are other genes involved in these pathways as well, some of the genes were selected based on the previously-described existing activities (*e.g., fadB1/4/5*) [30, 31, 37] or on the assumption that the studied genes could represent other genes in the same gene clusters, which are regulated by the same operons (*e.g., pqsA* as a representative of the *pqsABCDE* operon) [38–43]. In addition to these genes, expression levels of genes associated with the QS communication networks (*lasI, lasR, rhlI, rhlR, pqsR*) and a regulator of environmental stress responses, biofilm formation, and virulence (*rpoS*) [44, 45] were also examined.

To our surprise, exposure to 100 Hz acoustic vibration for 48 h downregulated only one out of the 27 target genes, *rhlA*, with statistical significance and a small magnitude of change (1.3-fold), whereas the rest of the genes did not exhibit significant differences between the two groups (Fig 4B). Hypothesized that the observed changes in metabolite levels might be the consequence of earlier changes in gene transcript expression levels, we carried out similar qRT-PCR analyses at 12 h after sound exposure, when the *P. aeruginosa* cultures had just entered stationary phase (see Fig 5). Interestingly, the results revealed statistically significant upregulation of three genes: *fabY* (1.5-fold), *fadE* (1.7-fold), and *pqsA* (1.4-fold). However, the changes in gene expression remained relatively small in magnitude, and the relative levels of other genes, including *rhlA*, appeared unaltered (Fig 4A). Together, the findings on gene expression levels supported the findings of metabolite levels in the metabolomics data.

Effects of oleic acid and rhamnolipids on the growth of *P. aeruginosa* under 100 Hz vibration

As the two main classes of metabolites with differential levels following 100 Hz sound exposure in extracellular samples were fatty acids and rhamnolipids (RLs), we evaluated the correlation between response and tolerance to acoustic vibration by testing the effects of these classes of metabolites on *P. aeruginosa* growth upon sound exposure by using sodium oleate (NaOA) as a representative of fatty acids, and a mixture of MRLs and DRLs for RLs. *P. aeruginosa* PAO1 was cultured under the same conditions as those for the metabolomics experiments but with or without supplementation of NaOA or RLs. However, because some cells were noticed to aggregate at the bottom of the cultured bottles at 24 h onwards, a behavior that might have consequences on bacterial growth, only 1 mL of PAO1 culture was grown in each culture vial, collected all at once at an indicated time point, and mixed vigorously to obtain homogeneous cultures before OD_{600} measurement. For the concentrations of treatment, it was reported that RLs blocked biofilm formation completely at a concentration of 250 μM [46]. Rationalized that higher concentrations might yield more prominent changes, we treated the cells with higher concentrations of NaOA and RLs at 2 mM and 10 mM. Please note that for RLs, these concentrations are equivalent to 1.2 g L^{-1} and 6.0 g L^{-1} when the average molecular weight of the mixture is assumed to be 600 g mol^{-1}.

Growth curves of *P. aeruginosa* cultures indicated that, in general, supplementation of NaOA into the culture resulted in significant increases in the cell densities of *P. aeruginosa* (Fig 5A and 5B). The increases were more prominent with a higher concentration of NaOA, with the cell densities continuing to increase to 24 h. At 24 h, NaOA-treated cultures grown in
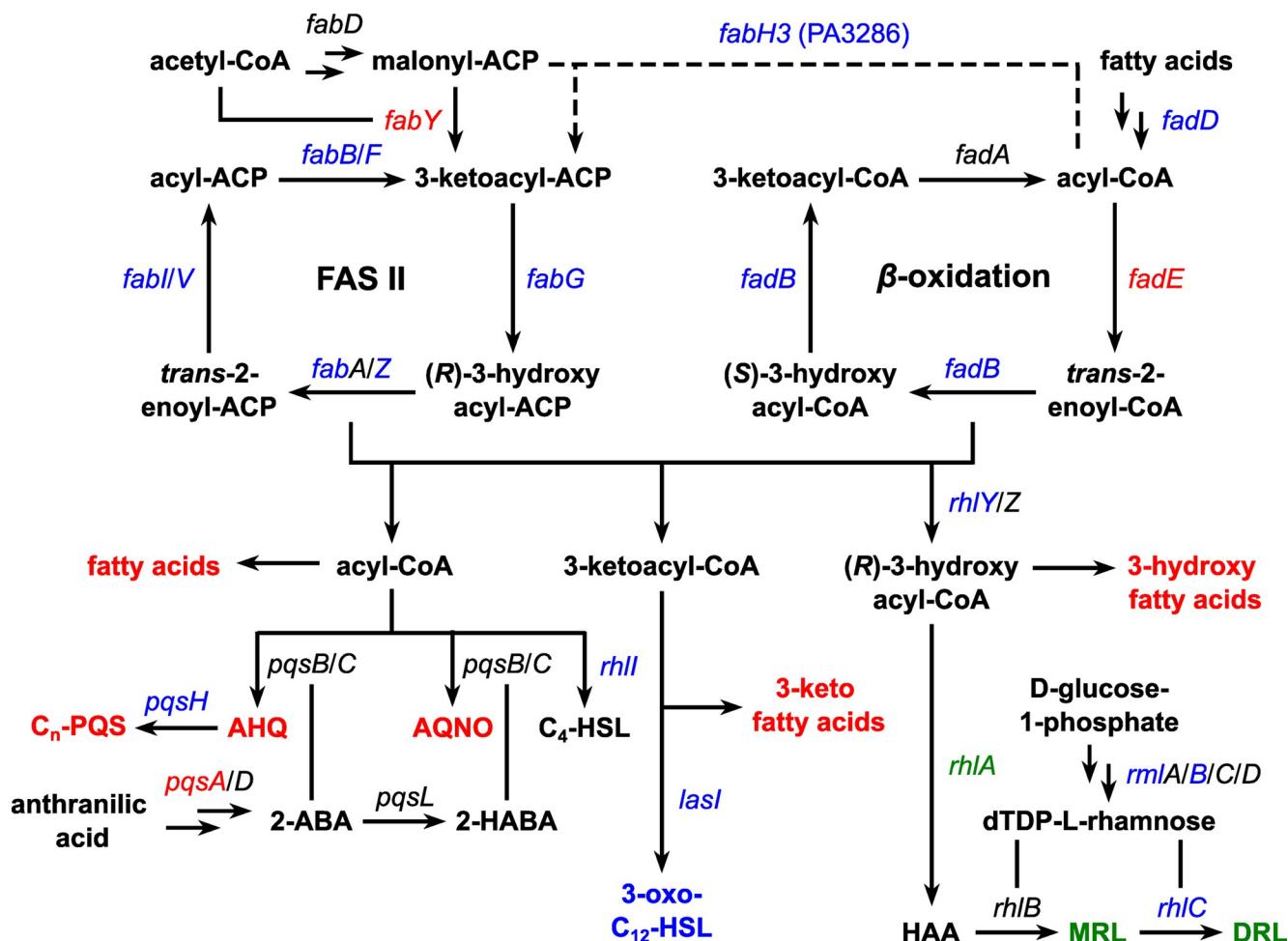
Fig 3. Biosynthetic pathways of differential and related metabolites in *Pseudomonas aeruginosa* and their interconnection. The key intermediates and enzyme-encoding genes are shown for the *de novo* fatty acid synthase (FAS II), β-oxidation, quinolones, *N*-acyl homoserine lactones, and rhamnolipids pathways. Metabolites or genes with elevated, decreased, or unchanged levels after 100-Hz sound exposure in the metabolomics analysis or quantitative real-time polymerase chain reaction are indicated by red, green, and blue letters, respectively. Abbreviations: 2-ABA, 2'-aminobenzoylacetate; 2-HABA, 2'-hydroxylaminobenzoylacetate; 3-oxo-C_{12}-HSL, *N*-(3-oxododecanoyl)-L-homoserine lactone; ACP, acyl carrier protein; AHQ, 2-alkyl-4-hydroxyquinoline; AQNO, 2-alkyl-4-hydroxyquinoline *N*-oxide; C_4-HSL, *N*-butyl-L-homoserine lactone; CoA, coenzyme A; C_n-PQS, 2-alkyl-3-hydroxy-4-quinolone; DRL, dirhamnolipid; HAA, 3-(3-hydroxyalkanoyloxy)alkanoic acid; MRL, monorhamnolipid.

https://doi.org/10.1371/journal.pone.0297030.g003

silence showed higher cell densities compared to those under 100-Hz vibration. However, the difference was only statistically significant with 2 mM NaOA cultures, and the magnitude of the difference was relatively small. At 48 h, the cell densities of silent NaOA cultures were found to decrease at both concentrations, whereas those of 100 Hz-exposed NaOA cultures appeared to increase slightly from previous time points, rendering their cell densities significantly different from their silent counterparts.

For RLs, no significant differences in growth were detected with 1.2 g L^{-1} RLs supplementation compared to untreated controls, with or without 100 Hz vibration treatment (Fig 5C). Nevertheless, with 6.0 g L^{-1} RLs supplementation, RLs slowed down the growth of *P. aeruginosa* with statistical significance at the beginning of incubation at 6 h, but the cell densities of the RLs cultures became higher than those of no-RLs controls at 24 h onward (Fig 5D). Unlike the cases of NaOA cultures, however, 100-Hz vibration did not alter the cell densities of RLs cultures compared to the no-vibration controls. Together, the data suggest that the elevation in
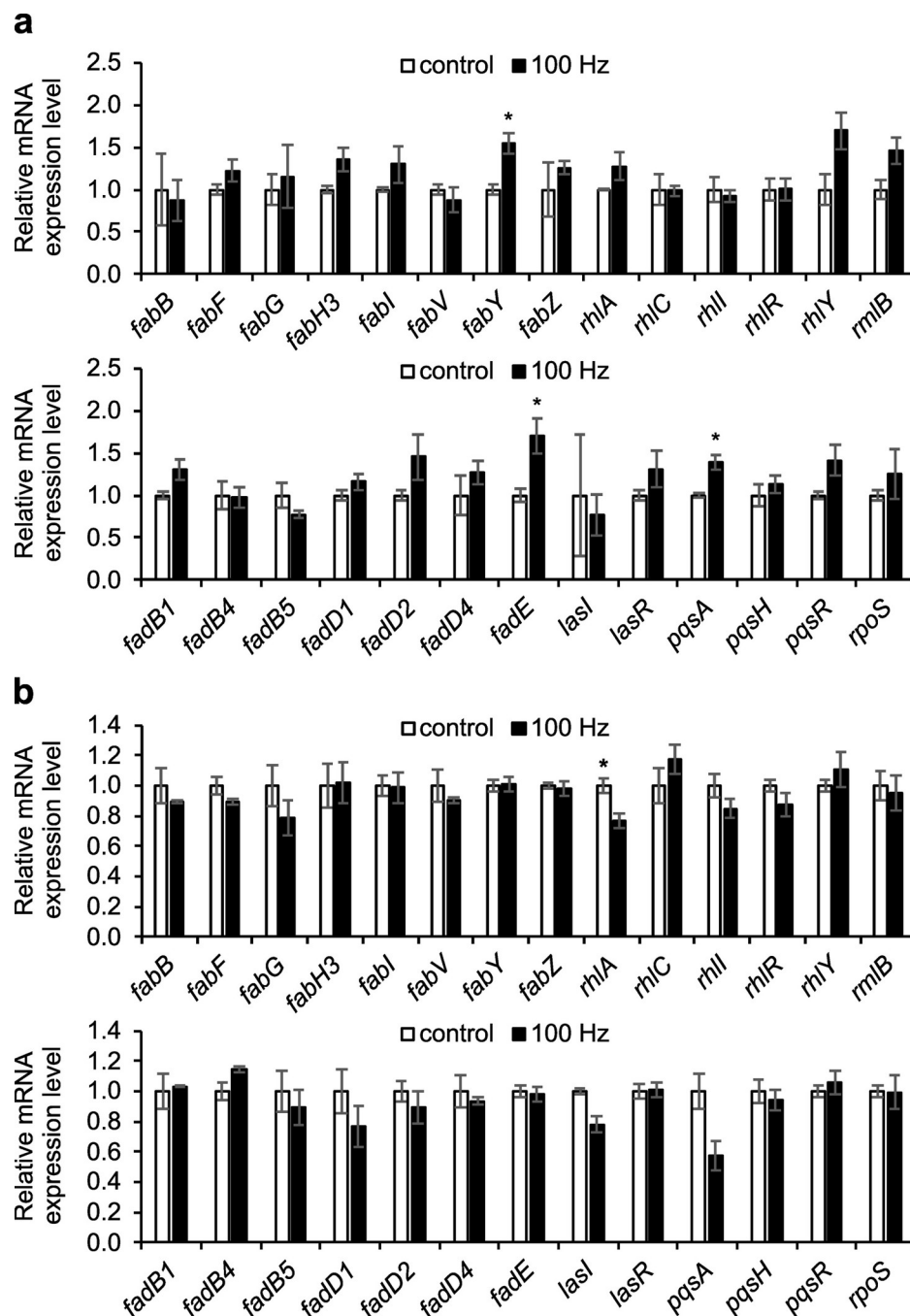
Fig 4. Relative transcript expression levels of genes involved in the biosynthesis of differential metabolites and related pathways in *Pseudomonas aeruginosa*. mRNA expression levels were quantitated in *Pseudomonas aeruginosa* at (a) 12 h and (b) 48 h after exposure to 100-Hz sound (100 Hz; black bars) and are indicated in the graph by normalizing the level of each gene with that of the control group without sound exposure (control; white bars). Quantitative real-time polymerase chain reaction was performed using the $2^{-\Delta\Delta Ct}$ method and standardized against the *rpoD* and *proC* transcript expression levels as internal controls. Data from three independent experiments are shown as the average ± standard errors of the mean. Student's *t*-test: *, $p < 0.05$.
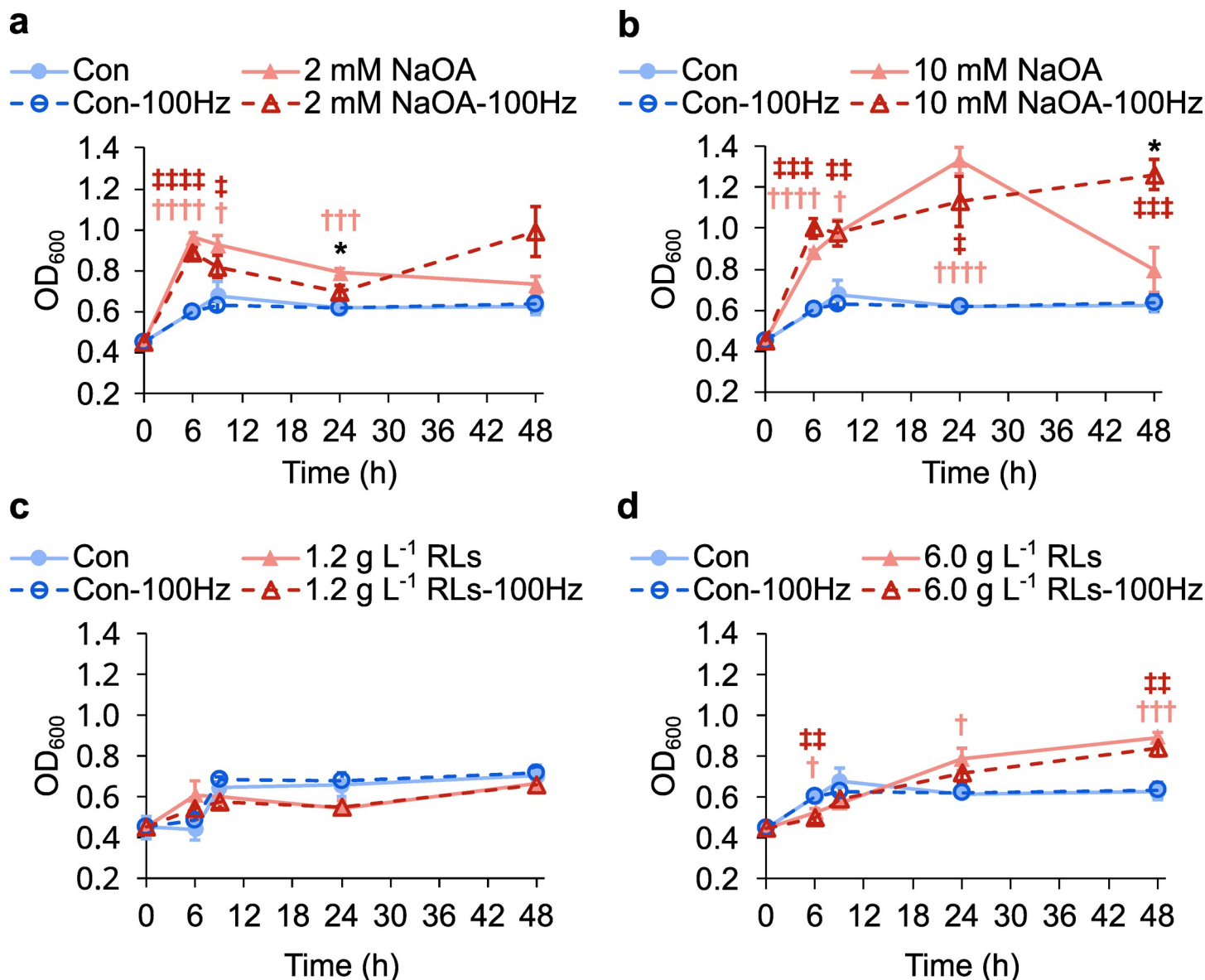
Fig 5. Acoustic vibration tolerance of *Pseudomonas aeruginosa* in the presence of response metabolites. Growth curves of *Pseudomonas aeruginosa* in the absence (control; Con; blue tone circle) or presence (red tone triangle) of (a) 2 mM sodium oleate (NaOA; 2 mM NaOA), (b) 10 mM NaOA, (c) 1.2 g L^{-1} rhamnolipids (RLs; 1.2 g L^{-1} RLs), or (d) 6.0 g L^{-1} RLs with (-100Hz; open marker with dashed line) or without (closed marker with solid line) stimulation by 100 Hz sound. One mL of cultures was collected at 6, 12, 24, or 48 h of incubation, mixed vigorously to obtain homogeneous culture, and subjected to optical density measurement at 600 nm (OD_{600}). Data from three or four independent cultures are shown as the average ± standard errors of the mean. Student's *t*-test for compound-treated samples with *vs.* without sound: [*], $p < 0.05$. Student's *t*-test for compound-treated *vs.* Con samples without sound: [†], $p < 0.05$; [††], $p < 0.01$; [†††], $p < 0.005$; [††††], $p < 0.001$. Student's *t*-test for compound-treated *vs.* Con samples with sound: [‡], $p < 0.05$; [‡‡], $p < 0.01$; [‡‡‡], $p < 0.005$; [‡‡‡‡], $p < 0.001$.

levels of fatty acids, especially oleic acid, when exposed to 100-Hz acoustic vibration might play a role in maintaining the cell densities of *P. aeruginosa* at heightened levels for a longer period and support the correlation between the response and tolerance of *P. aeruginosa* to acoustic vibration.

Discussion

Sound is an integral part of every environment, and its impact on living organisms has been the subject of extensive research. Studies have shown that sound, including music, can have positive effects on various living organisms, such as reducing stress, promoting embryonic development, and improving immune responses in humans, chicks, mice, and rats [47]. In plants, sound vibrations have been found to enhance crop yield, improve photosynthesis, increase tolerance to drought stress, influence hormone levels, and affect root growth and bending, as well as gene and protein expression related to defense and photosynthesis [48]. However, the effects of sound on bacteria, especially at the molecular level, have been limited, despite their significance in medical health and industrial applications. Therefore, in this study, we investigated the effects of 100 Hz acoustic vibration on *Pseudomonas aeruginosa* using untargeted metabolomics approaches to gain insights into the molecular-level impact of sound on bacteria.

In our study, *P. aeruginosa* was exposed to 100-Hz acoustic vibration in NB medium for 48 h, a condition previously reported to enhance biofilm formation by 0.3-fold compared to the silence control [13]. Interestingly, we did not observe any biofilm at all in our cases. The main differences between the two studies were the culture temperatures (30˚C *vs*. 37˚C) and the culture containers (culture glass bottle and vial *vs*. Petri dish). Previous research using the PAO1 strain of *P. aeruginosa* showed that biofilm formation was highest at 20˚C, lowest at 25˚C, and gradually increased again at higher temperatures, from 25˚C to 30˚C to 37˚C [49]. The 30˚C culture temperature employed in this study, which mimics the environmental condition, could thus reduce the amount of biofilm formation compared to the 37˚C culture temperature in the previous study. Yet, in our view, the effects of temperature may be smaller compared to the effects of culture containers, as we could notice a small layer of biofilm at the air-liquid interface in all cultures when using a different type of culture tube in a separate but similar independent experiment.

As mentioned earlier, acoustic vibration has the potential to alter the growth of various microorganisms. However, a previous report on *P. aeruginosa* exposed to 800-Hz vibration showed increased bacterial cell numbers only in biofilm, but not in planktonic cells [13]. In our study, the growth of *P. aeruginosa* under 100-Hz sound treatment did not show significant differences compared to the silent control. As we observed only aggregates in our cultures, not biofilm, it is possible that *P. aeruginosa* cultures in our study may exhibit growth behaviors similar to planktonic cells, with unchanged cell numbers as previously described.

The untargeted metabolomics analysis of *P. aeruginosa* under 100-Hz sound treatment showed elevated levels of fatty acids, quinolones, and NAE, but depleted levels of RLs, compared to the silent control. RLs are a biosurfactant, which plays a crucial role in promoting biofilm formation in *P. aeruginosa*. In the early stages of biofilm development, a small amount of RLs increases the hydrophobicity of cells, facilitating their attachment to the surface. As the biofilm matures, a high concentration of RLs inhibits cell attachment and microcolony formation, maintaining the complex architecture of the biofilm and enabling the seeding dispersal of motile cells [50, 51]. Thus, reducing the levels of RLs under 100-Hz vibration exposure as detected here should enhance biofilm formation, which aligns with the effects found in the previous report [13]. Fatty acids (*i.e*., linoleic acid) and quinolones (*i.e*., synthetic fluoroquinolones) were demonstrated to promote biofilm dispersion as well [52, 53]. However, because their levels were increased upon sound exposure in this case, they would exert contradictory effects to those of decreasing RLs. It is therefore plausible that the observed increases in the levels of fatty acids and quinolones were simply artifacts resulting from the lower production of

RLs, which left more of their precursors, *i.e.*, free fatty acids, around and available for conversion into quinolones.

In fact, the qRT-PCR results (Fig 4) provide evidence for the correlation between the levels of RLs, fatty acids, and quinolones. The synthesis of RL involves the conversion of (*R*)-3-hydroxyacyl-CoA to 3-(3-hydroxyalkanoyloxy)alkanoic acid (HAA), the process catalyzed by RhlA. HAA then undergoes catalytic transformation by RhlB and RhlC to produce MRL and DRL, respectively (Fig 3) [29, 42, 54, 55]. Following exposure to 100-Hz vibration for 48 h, the level of *rhlA* gene was slightly but significantly reduced, compared to the unexposed control. This downregulation could potentially result in a decrease in the levels of RL products and an accumulation of (*R*)-3-hydroxyacyl-CoA and its precursors, thereby leading to the increase in the levels of fatty acids and quinolones. Notably, no changes in the level of *rhlA* gene were observed at the earlier time point of 12 h, indicating that the alteration in RL levels may occur only during the late stationary phase.

The effects of 100-Hz vibration exposure on gene expression were not limited to changes in the *rhlA* gene at 48 h, but also included significant upregulation of *fabY*, *fadE*, and *pqsA* genes at 12 h. FabY and FadE play critical roles in the *de novo* fatty acid synthesis (FAS II) and fatty acid *β*-oxidation pathways, respectively. FabY initiates the FAS II pathway by catalyzing the reaction between malonyl-ACP and acetyl-CoA to produce 3-ketoacyl-ACP [56], while FadE converts acyl-CoA to enoyl-CoA molecule, thereby starting off the *β*-oxidation pathway to break down long-chain fatty acids to those with shorter fatty acyl chains required for PQS and other quinolones syntheses [31]. In fact, previous studies have demonstrated that the PQS level was increased only in the presence of FadE when supplementing *P. aeruginosa* cultures with oleic acid (FA(18:1)), indicating that these two enzymes may contribute to the observed accumulation of fatty acids and quinolones upon vibration exposure. Additionally, PqsA catalyzes the conversion of anthranilic acid, a precursor in the biosynthesis of quinolones [21, 57]. The upregulation of *pqsA* gene expression may thus represent another factor directly contributing to the increased production of quinolones upon vibration exposure.

We also examined the impact of acoustic vibration on the regulator that is involved in environmental stress responses, biofilm formation, and virulence, as well as the QS networks that control RLs and quinolones. Specifically, we analyzed the levels of *rpoS* gene and the genes in these networks, such as lasI/R genes for the Las system, rhlI/R genes for the Rhl system, and pqsR gene for the PQS system [16, 44, 45]. Our results showed no significant changes in these transcript levels or in the product of LasI, 3-oxo-C_{12}-HSL, indicating no association between the acoustic vibration, the regulator, and the Las and Rhl systems. However, we observed an increase in intracellular levels of quinolones other than PQS, suggesting the potential involvement of the PQS system in the response to the vibration. Nonetheless, additional mechanistic studies are necessary to elucidate the regulatory mechanisms behind these changes and their implications for the organism.

Upon exposure to 100-Hz vibration, another class of metabolites that shows an increase in intracellular levels is NAE. NAEs are naturally occurring molecules derived from fatty acids that act as signaling molecules in various physiological processes in animals and plants. They are involved in inflammation, metabolism, and stress response [58, 59]. The biosynthesis of NAEs can be initiated from phosphatidylethanolamine (PE), a phospholipid that is abundant in cell membranes. This involves the acylation of PE to *N*-acylphosphatidylethanolamine, which is then cleaved to form NAE. Alternatively, studies have described the enzymatic formation of NAE from fatty acids and ethanolamine [60], which is derived from PE through phosphodiesterases. Our study did not detect any change in the levels of PE under 100-Hz vibration treatment, implying that the availability of ethanolamine might be similar in both sound-treated and untreated conditions. Nevertheless, the elevated levels of fatty acids during

sound exposure could potentially result in an increase in NAE levels, as supported by previous findings that have suggested a correlation between plasma NAE and fatty acid levels in women [61]. It should be noted, however, that there is currently no information available on the roles or biosynthesis of NAE in *P. aeruginosa*. Therefore, further investigation is needed to determine how changes in NAE levels affect *P. aeruginosa*.

In this study, two classes of metabolites, namely fatty acids and RLs, were observed to exhibit increased and decreased extracellular levels, respectively, upon exposure to 100-Hz acoustic vibration. From an evolutionary perspective, organisms may produce responses to protect against stress and enhance cell tolerance [1]. Accordingly, adding fatty acids to the culture media, which would mimic the observed change, may improve cell survival under sound exposure, while adding RL mixtures, which oppose the observed change, may sensitize cells. This hypothesis was supported by the growth of *P. aeruginosa* in sodium oleate under acoustic vibration treatment, which remained the only culture with heightened cell densities at 48 h. In general, the cell densities of *P. aeruginosa* in sodium oleate were also increased compared to the no-compound control, potentially serving as nutrients by entering through the β-oxidation pathway [30]. Interestingly, the lack of growth changes upon RL supplementation suggests that the response may be a general one, unrelated to *P. aeruginosa*'s survival and tolerance to sound, or the changes in RL levels may affect other physiological conditions not assessed in this study.

Conclusions

In summary, we utilized untargeted metabolomics analysis to investigate the effects of 100-Hz acoustic vibration on the hydrophobic metabolites of *P. aeruginosa* PAO1, both intra- and extracellularly. Our analysis revealed alterations in the levels of 111 metabolite ions, of which 75% were assigned probable structures using accurate masses, retention time, tandem mass spectra, and some synthetic standards. Fatty acids and their derivatives, quinolones, and NAEs showed increased levels upon sound exposure, while RLs were decreased. qRT-PCR experiments indicated the slight downregulation of RL biosynthetic genes and upregulation of fatty acid and quinolone biosynthetic genes, but no significant changes in the regulator or QS network genes were observed. Furthermore, sodium oleate, a representative fatty acid, was found to enhance the tolerance of *P. aeruginosa* in the presence of acoustic stimulation at 48 h. For the first time, these findings shed light on the ways in which mechanical vibrations affect bacterial metabolism, physiology, and gene expression, with potential implications for controlling bacterial infections. Future work will aim to further elucidate the involved mechanisms, especially at the regulatory and mechanotransduction levels, apply the studies to clinical or other strains of *P. aeruginosa* under environments conducive to biofilm formation, and extend these methods to study other bacteria for medical, agricultural, and industrial applications.

Supporting information

S1 File. S1–S10 Tables and S1 Fig. S1–S7 Tables. Significantly increased or decreased positive-mode or negative-mode ions in 100-Hz-treated *P. aeruginosa* extracellular or intracellular samples compared to the no-sound control in the metabolomics analysis. S8 Table. Levels of other known metabolites in 100-Hz-treated *P. aeruginosa* extracellular and intracellular samples compared to the no-sound control in the metabolomics analysis. S9 Table. List of metabolite standards with MS/MS spectra in the positive and negative ion modes. S10 Table. Oligonucleotides used as forward and reverse primers for amplification of target genes in the quantitative real-time polymerase chain reaction. S1 Fig. List of MS/MS Spectra.
(PDF)

Acknowledgments

Author Contributions

Conceptualization: Nawaporn Vinayavekhin, Mark Francis Murphy.

Formal analysis: Nawaporn Vinayavekhin.

Investigation: Nawaporn Vinayavekhin, Thanyaporn Wattanophas.

Resources: Mark Francis Murphy, Alisa S. Vangnai, Glyn Hobbs.

Supervision: Nawaporn Vinayavekhin, Mark Francis Murphy.

Visualization: Nawaporn Vinayavekhin, Thanyaporn Wattanophas.

Writing – original draft: Nawaporn Vinayavekhin.

Writing – review & editing: Nawaporn Vinayavekhin, Mark Francis Murphy, Alisa S. Vangnai, Glyn Hobbs.

References

1. Nicolaou SA, Gaida SM, Papoutsakis ET. A comparative view of metabolite and substrate stress and tolerance in microbial bioprocessing: From biofuels and chemicals, to biocatalysis and bioremediation. Metab Eng. 2010; 12(4):307–31. Epub https://doi.org/10.1016/j.ymben.2010.03.004 PMID: 20346409.

2. Sharma SC, Arino J, Pascual-Ahuir A, Mulet JM, Mazzoni C. Editorial: microbial stress responses: anti-oxidants, the plasma membrane, and beyond. Front Microbiol. 2022; 13. https://doi.org/10.3389/fmicb.2022.891964 PMID: 35722293

3. Bassler BL. Small talk: Cell-to-cell communication in bacteria. Cell. 2002; 109(4):421–4. https://doi.org/10.1016/S0092-8674(02)00749-3

4. Armitage JP. Behavioural responses of bacteria to light and oxygen. Arch Microbiol. 1997; 168(4):249–61. https://doi.org/10.1007/s002030050496 PMID: 9297461

5. Shapiro RS, Cowen LE. Thermal control of microbial development and virulence: molecular mechanisms of microbial temperature sensing. mBio. 2012; 3(5). Epub https://doi.org/10.1128/mBio.00238-12 PMID: 23033469.

6. Kumawat C, Kumar A, Parshad J, Sharma SS, Patra A, Dogra P, et al. Microbial diversity and adaptation under salt-affected soils: a review. Sustainability. 2022; 14(15). https://doi.org/10.3390/su14159280

7. Guan N, Liu L. Microbial response to acid stress: mechanisms and applications. Appl Microbiol Biotechnol. 2020; 104(1):51–65. Epub https://doi.org/10.1007/s00253-019-10226-1 PMID: 31773206.

8. Frimmersdorf E, Horatzek S, Pelnikevich A, Wiehlmann L, Schomburg D. How *Pseudomonas aeruginosa* adapts to various environments: a metabolomic approach. Environ Microbiol. 2010; 12(6):1734–47. https://doi.org/10.1111/j.1462-2920.2010.02253.x PMID: 20553553

9. Sarvaiya N, Kothari V. Effect of audible sound in form of music on microbial growth and production of certain important metabolites. Microbiology. 2015; 84(2):227–35. https://doi.org/10.1134/S0026261715020125

10. Gu S, Zhang Y, Wu Y. Effects of sound exposure on the growth and intracellular macromolecular synthesis of *E. coli* k-12. PeerJ. 2016; 4:e1920. Epub https://doi.org/10.7717/peerj.1920

11. Aggio RBM, Obolonkin V, Villas-Bôas SG. Sonic vibration affects the metabolism of yeast cells growing in liquid culture: a metabolomic study. Metabolomics. 2012; 8(4):670–8. https://doi.org/10.1007/s11306-011-0360-x

12. Harris A, Lindsay MA, Ganley ARD, Jeffs A, Villas-Boas SG. Sound stimulation can affect *Saccharomyces cerevisiae* growth and production of volatile metabolites in liquid medium. Metabolites. 2021; 11(9). Epub https://doi.org/10.3390/metabo11090605

13. Murphy MF, Edwards T, Hobbs G, Shepherd J, Bezombes F. Acoustic vibration can enhance bacterial biofilm formation. J Biosci Bioeng. 2016; 122(6):765–70. Epub https://doi.org/10.1016/j.jbiosc.2016.05.010 PMID: 27338651.

14. Centers for Disease Control and Prevention. *Pseudomonas aeruginosa* in Healthcare Settings. 2019 Nov 13 [cited 13 February 2023]. Available from: https://www.cdc.gov/hai/organisms/pseudomonas.html.

15. Qin S, Xiao W, Zhou C, Pu Q, Deng X, Lan L, et al. *Pseudomonas aeruginosa*: pathogenesis, virulence factors, antibiotic resistance, interaction with host, technology advances and emerging therapeutics. Signal Transduction Targeted Ther. 2022; 7(1):199. https://doi.org/10.1038/s41392-022-01056-1 PMID: 35752612

16. Williams P, Cámara M. Quorum sensing and environmental adaptation in *Pseudomonas aeruginosa*: a tale of regulatory networks and multifunctional signal molecules. Curr Opin Microbiol. 2009; 12(2):182–91. https://doi.org/10.1016/j.mib.2009.01.005.

17. Jones S, Yu B, Bainton NJ, Birdsall M, Bycroft BW, Chhabra SR, et al. The lux autoinducer regulates the production of exoenzyme virulence determinants in *Erwinia carotovora* and *Pseudomonas aeruginosa*. EMBO J. 1993; 12(6):2477–82. https://doi.org/10.1002/j.1460-2075.1993.tb05902.x PMID: 8508773

18. Pearson JP, Gray KM, Passador L, Tucker KD, Eberhard A, Iglewski BH, et al. Structure of the autoinducer required for expression of *Pseudomonas aeruginosa* virulence genes. Proc Natl Acad Sci U S A. 1994; 91(1):197–201. https://doi.org/10.1073/pnas.91.1.197 PMID: 8278364

19. Ochsner UA, Reiser J. Autoinducer-mediated regulation of rhamnolipid biosurfactant synthesis in *Pseudomonas aeruginosa*. Proc Natl Acad Sci U S A. 1995; 92(14):6424–8. https://doi.org/10.1073/pnas.92.14.6424 PMID: 7604006

20. Pearson JP, Passador L, Iglewski BH, Greenberg EP. A second *N*-acylhomoserine lactone signal produced by *Pseudomonas aeruginosa*. Proc Natl Acad Sci U S A. 1995; 92(5):1490–4. https://doi.org/10.1073/pnas.92.5.1490 PMID: 7878006

21. Gallagher LA, McKnight SL, Kuznetsova MS, Pesci EC, Manoil C. Functions required for extracellular quinolone signaling by *Pseudomonas aeruginosa*. J Bacteriol. 2002; 184(23):6472–80. https://doi.org/10.1128/jb.184.23.6472–6480.2002

22. Pesci EC, Milbank JB, Pearson JP, McKnight S, Kende AS, Greenberg EP, et al. Quinolone signaling in the cell-to-cell communication system of *Pseudomonas aeruginosa*. Proc Natl Acad Sci U S A. 1999; 96 (20):11229–34. https://doi.org/10.1073/pnas.96.20.11229 PMID: 10500159

23. Venturi V. Regulation of quorum sensing in *Pseudomonas*. FEMS Microbiol Rev. 2006; 30(2):274–91. https://doi.org/10.1111/j.1574-6976.2005.00012.x PMID: 16472307

24. Schrimpe-Rutledge AC, Codreanu SG, Sherrod SD, McLean JA. Untargeted metabolomics strategies-challenges and emerging directions. J Am Soc Mass Spectrom. 2016; 27(12):1897–905. Epub https://doi.org/10.1007/s13361-016-1469-y PMID: 27624161.

25. Vinayavekhin N, Kongchai W, Piapukiew J, Chavasiri W. *Aspergillus niger* upregulated glycerolipid metabolism and ethanol utilization pathway under ethanol stress. MicrobiologyOpen. 2020; 9(1): e00948. Epub https://doi.org/10.1002/mbo3.948

26. Vinayavekhin N, Mahipant G, Vangnai AS, Sangvanich P. Untargeted metabolomics analysis revealed changes in the composition of glycerolipids and phospholipids in *Bacillus subtilis* under 1-butanol stress. Appl Microbiol Biotechnol. 2015; 99(14):5971–83. Epub https://doi.org/10.1007/s00253-015-6692-0

27. Savli H, Karadenizli A, Kolayli F, Gundes S, Ozbek U, Vahaboglu H. Expression stability of six housekeeping genes: A proposal for resistance gene quantification studies of *Pseudomonas aeruginosa* by real-time quantitative RT-PCR. J Med Microbiol. 2003; 52(Pt 5):403–8. https://doi.org/10.1099/jmm.0.05132–0

28. Smith CA, Want EJ, O'Maille G, Abagyan R, Siuzdak G. XCMS: processing mass spectrometry data for metabolite profiling using nonlinear peak alignment, matching, and identification. Anal Chem. 2006; 78 (3):779–87. https://doi.org/10.1021/ac051437y PMID: 16448051

29. Abdel-Mawgoud AM, Lépine F, Déziel E. A stereospecific pathway diverts β-oxidation intermediates to the biosynthesis of rhamnolipid biosurfactants. Chem Biol. 2014; 21(1):156–64. Epub https://doi.org/10.1016/j.chembiol.2013.11.010

30. Sun Z, Kang Y, Norris MH, Troyer RM, Son MS, Schweizer HP, et al. Blocking phosphatidylcholine utilization in *Pseudomonas aeruginosa*, via mutagenesis of fatty acid, glycerol and choline degradation pathways, confirms the importance of this nutrient source in vivo. PLoS One. 2014; 9(7):e103778. https://doi.org/10.1371/journal.pone.0103778 PMID: 25068317

31. Wells G, Palethorpe S, Pesci EC. PsrA controls the synthesis of the *Pseudomonas aeruginosa* quinolone signal via repression of the FadE homolog, PA0506. PLoS One. 2017; 12(12):e0189331. https://doi.org/10.1371/journal.pone.0189331 PMID: 29220387

32. Zhang L, Veres-Schalnat TA, Somogyi A, Pemberton JE, Maier RM. Fatty acid cosubstrates provide *β*-oxidation precursors for rhamnolipid biosynthesis in *Pseudomonas aeruginosa*, as evidenced by isotope tracing and gene expression assays. Appl Environ Microbiol. 2012; 78(24):8611–22. Epub https://doi.org/10.1128/aem.02111-12

33. Déziel E, Lépine F, Milot S, He J, Mindrinos MN, Tompkins RG, et al. Analysis of *Pseudomonas aeruginosa* 4-hydroxy-2-alkylquinolines (HAQs) reveals a role for 4-hydroxy-2-heptylquinoline in cell-to-cell communication. Proc Natl Acad Sci U S A. 2004; 101(5):1339–44. Epub https://doi.org/10.1073/pnas.0307694100

34. Yuan Y, Leeds JA, Meredith TC. *Pseudomonas aeruginosa* directly shunts *β*-oxidation degradation intermediates into de novo fatty acid biosynthesis. J Bacteriol. 2012; 194(19):5185–96. Epub https://doi.org/10.1128/jb.00860-12

35. Zhu L, Lin J, Ma J, Cronan JE, Wang H. Triclosan resistance of *Pseudomonas aeruginosa* PAO1 is due to FabV, a triclosan-resistant enoyl-acyl carrier protein reductase. Antimicrob Agents Chemother. 2010; 54(2):689–98. Epub https://doi.org/10.1128/aac.01152-09

36. Winsor GL, Griffiths EJ, Lo R, Dhillon BK, Shay JA, Brinkman FS. Enhanced annotations and features for comparing thousands of *Pseudomonas* genomes in the Pseudomonas genome database. Nucleic Acids Res. 2016; 44(D1):D646–53. Epub https://doi.org/10.1093/nar/gkv1227

37. Son MS, Matthews WJ, Jr., Kang Y, Nguyen DT, Hoang TT. In vivo evidence of *Pseudomonas aeruginosa* nutrient acquisition and pathogenesis in the lungs of cystic fibrosis patients. Infect Immun. 2007; 75(11):5313–24. Epub https://doi.org/10.1128/iai.01807-06

38. Aguirre-Ramírez M, Medina G, González-Valdez A, Grosso-Becerra V, Soberón-Chávez G. The *Pseudomonas aeruginosa rmlBDAC* operon, encoding dTDP-L-rhamnose biosynthetic enzymes, is regulated by the quorum-sensing transcriptional regulator RhlR and the alternative sigma factor σS. Microbiology (Reading). 2012; 158(Pt 4):908–16. Epub https://doi.org/10.1099/mic.0.054726–0

39. Boechat AL, Kaihami GH, Politi MJ, Lépine F, Baldini RL. A novel role for an ECF sigma factor in fatty acid biosynthesis and membrane fluidity in *Pseudomonas aeruginosa*. PLoS One. 2013; 8(12):e84775. Epub https://doi.org/10.1371/journal.pone.0084775

40. Hoang TT, Schweizer HP. Fatty acid biosynthesis in *Pseudomonas aeruginosa*: cloning and characterization of the *fabAB* operon encoding beta-hydroxyacyl-acyl carrier protein dehydratase (FabA) and beta-ketoacyl-acyl carrier protein synthase I (FabB). J Bacteriol. 1997; 179(17):5326–32. https://doi.org/10.1128/jb.179.17.5326–5332.1997

41. Soberón-Chávez G, González-Valdez A, Soto-Aceves MP, Cocotl-Yañez M. Rhamnolipids produced by *Pseudomonas*: from molecular genetics to the market. Microb Biotechnol. 2021; 14(1):136–46. Epub https://doi.org/10.1111/1751-7915.13700

42. Ochsner UA, Fiechter A, Reiser J. Isolation, characterization, and expression in *Escherichia coli* of the *Pseudomonas aeruginosa rhlAB* genes encoding a rhamnosyltransferase involved in rhamnolipid biosurfactant synthesis. J Biol Chem. 1994; 269(31):19787–95.

43. Brouwer S, Pustelny C, Ritter C, Klinkert B, Narberhaus F, Häussler S. The PqsR and RhlR transcriptional regulators determine the level of *Pseudomonas* quinolone signal synthesis in *Pseudomonas aeruginosa* by producing two different *pqsABCDE* mRNA isoforms. J Bacteriol. 2014; 196(23):4163–71. Epub https://doi.org/10.1128/jb.02000-14

44. Duan X, Pan Y, Cai Z, Liu Y, Zhang Y, Liu M, et al. *rpoS*-mutation variants are selected in *Pseudomonas aeruginosa* biofilms under imipenem pressure. Cell Biosci. 2021; 11(1):138. https://doi.org/10.1186/s13578-021-00655-9 PMID: 34289907

45. Schuster M, Hawkins AC, Harwood CS, Greenberg EP. The *Pseudomonas aeruginosa* RpoS regulon and its relationship to quorum sensing. Mol Microbiol. 2004; 51(4):973–85. https://doi.org/10.1046/j.1365-2958.2003.03886.x PMID: 14763974

46. Davey ME, Caiazza NC, O'Toole GA. Rhamnolipid surfactant production affects biofilm architecture in *Pseudomonas aeruginosa* PAO1. J Bacteriol. 2003; 185(3):1027–36. https://doi.org/10.1128/jb.185.3.1027–1036.2003

47. Exbrayat J-M, Brun C. Some effects of sound and music on organisms and cells: a review. Annu Res Rev Biol. 2019; 32(2):1–12. https://doi.org/10.9734/arrb/2019/v32i230080.

48. Jung J, Kim S-K, Kim JY, Jeong M-J, Ryu C-M. Beyond chemical triggers: evidence for sound-evoked physiological reactions in plants. Front Plant Sci. 2018; 9. https://doi.org/10.3389/fpls.2018.00025 PMID: 29441077

49. Kim S, Li XH, Hwang HJ, Lee JH. Thermoregulation of *Pseudomonas aeruginosa* biofilm formation. Appl Environ Microbiol. 2020; 86(22). Epub https://doi.org/10.1128/aem.01584-20

50. Nickzad A, Déziel E. The involvement of rhamnolipids in microbial cell adhesion and biofilm development—an approach for control? Lett Appl Microbiol. 2014; 58(5):447–53. Epub https://doi.org/10.1111/lam.12211 PMID: 24372465.

51. de Kievit TR. Quorum sensing in *Pseudomonas aeruginosa* biofilms. Environ Microbiol. 2009; 11 (2):279–88. https://doi.org/10.1111/j.1462-2920.2008.01792.x PMID: 19196266

52. Kim HS, Cha E, Ham SY, Park JH, Nam S, Kwon H, et al. Linoleic acid inhibits *Pseudomonas aeruginosa* biofilm formation by activating diffusible signal factor-mediated quorum sensing. Biotechnol Bioeng. 2021; 118(1):82–93. Epub https://doi.org/10.1002/bit.27552

53. Yassien M, Khardori N, Ahmedy A, Toama M. Modulation of biofilms of *Pseudomonas aeruginosa* by quinolones. Antimicrob Agents Chemother. 1995; 39(10):2262–8. https://doi.org/10.1128/aac.39.10.2262 PMID: 8619580

54. Déziel E, Lépine F, Milot S, Villemur R. *rhlA* is required for the production of a novel biosurfactant promoting swarming motility in *Pseudomonas aeruginosa*: 3-(3-hydroxyalkanoyloxy)alkanoic acids (HAAs), the precursors of rhamnolipids. Microbiology (Reading). 2003; 149(Pt 8):2005–13. https://doi.org/10.1099/mic.0.26154–0

55. Rahim R, Ochsner UA, Olvera C, Graninger M, Messner P, Lam JS, et al. Cloning and functional characterization of the *Pseudomonas aeruginosa rhlC* gene that encodes rhamnosyltransferase 2, an enzyme responsible for di-rhamnolipid biosynthesis. Mol Microbiol. 2001; 40(3):708–18. https://doi.org/10.1046/j.1365-2958.2001.02420.x PMID: 11359576

56. Yuan Y, Sachdeva M, Leeds JA, Meredith TC. Fatty acid biosynthesis in *Pseudomonas aeruginosa* is initiated by the FabY class of β-ketoacyl acyl carrier protein synthases. J Bacteriol. 2012; 194 (19):5171–84. https://doi.org/10.1128/jb.00792-12 PMID: 22753059

57. Calfee MW, Coleman JP, Pesci EC. Interference with Pseudomonas quinolone signal synthesis inhibits virulence factor expression by *Pseudomonas aeruginosa*. Proc Natl Acad Sci U S A. 2001; 98 (20):11633–7. https://doi.org/10.1073/pnas.201328498 PMID: 11573001

58. Blancaflor EB, Kilaru A, Keereetaweep J, Khan BR, Faure L, Chapman KD. *N*-Acylethanolamines: lipid metabolites with functions in plant growth and development. Plant J. 2014; 79(4):568–83. Epub https://doi.org/10.1111/tpj.12427

59. Mock ED, Gagestein B, van der Stelt M. Anandamide and other *N*-acylethanolamines: A class of signaling lipids with therapeutic opportunities. Prog Lipid Res. 2023; 89:101194. Epub https://doi.org/10.1016/j.plipres.2022.101194

60. Sugiura T, Kobayashi Y, Oka S, Waku K. Biosynthesis and degradation of anandamide and 2-arachidonoylglycerol and their possible physiological significance. Prostaglandins Leukot Essent Fatty Acids. 2002; 66(2–3):173–92. https://doi.org/10.1054/plef.2001.0356 PMID: 12052034

61. Joosten MM, Balvers MG, Verhoeckx KC, Hendriks HF, Witkamp RF. Plasma anandamide and other *N*-acylethanolamines are correlated with their corresponding free fatty acid levels under both fasting and non-fasting conditions in women. Nutr Metab (Lond). 2010; 7:49. Epub https://doi.org/10.1186/1743-7075-7-49